

## Synthesis of $\text{LiMnPO}_4/\text{C}$ composite material for lithium ion batteries by sol–gel method

ZHONG Sheng-kui<sup>1,2,3</sup>, WANG You<sup>2</sup>, LIU Jie-qun<sup>1,2,3</sup>, WANG Jian<sup>2</sup>

1. Guangxi Key Laboratory of New Energy and Building Energy Saving, Guilin University of Technology, Guilin 541004, China;
2. College of Chemistry and Bioengineering, Guilin University of Technology, Guilin 541004, China;
3. Shagang School of Iron and Steel, Soochow University, Suzhou 215021, China

Received 9 July 2012; accepted 1 August 2012

**Abstract:** The  $\text{LiMnPO}_4/\text{C}$  composite material was synthesized via a sol–gel method based on the citric acid. The X-ray diffraction (XRD), scanning electron microscopy (SEM) and electrochemical performance tests were adopted to characterize the properties of  $\text{LiMnPO}_4/\text{C}$ . The XRD studies show that the pure olivine phase  $\text{LiMnPO}_4$  can be obtained at a low temperature of 500 °C. The SEM analyses illustrate that the citric acid used as the chelating reagent and carbon source can restrain the particle size of  $\text{LiMnPO}_4/\text{C}$  well. The  $\text{LiMnPO}_4/\text{C}$  sample synthesized at 500 °C for 10 h performs the highest initial discharge capacity of 122.6 mA·h/g, retaining 112.4 mA·h/g over 30 cycles at 0.05C rate. The citric acid based sol–gel method is favor to obtain the high electrochemical performance of  $\text{LiMnPO}_4/\text{C}$ .

**Key words:** lithium-ion battery; cathode material; sol–gel method;  $\text{LiMnPO}_4/\text{C}$ ; electrochemical performance

### 1 Introduction

Polyanion compounds  $\text{LiMPO}_4$  (M=Mn, Fe, Co and Ni) are considered the promising cathode materials for lithium ion batteries.  $\text{LiMPO}_4$  (M=Mn, Fe, Co and Ni) cathode materials have more advantages than traditional materials, such as low cost and toxicity [1–3]. The high electrochemical and thermal stabilities of  $\text{LiMPO}_4$  are attributed to their phosphate structure [4,5]. In these compounds,  $\text{LiFePO}_4$  has received a wide application. Recently, much attention has been paid to  $\text{LiMnPO}_4$ , because of its high voltage platform of 4.1 V. Compared with  $\text{LiFePO}_4$ , the theoretical energy density of  $\text{LiMnPO}_4$  is about 1.2 times larger than that of the former [6]. However,  $\text{LiMnPO}_4$  presents a poor electrochemical performance, which is attributed to difficulty in lithium ion diffusion and low electronic conductivity [7,8]. To these disadvantages of  $\text{LiMnPO}_4$ , one effective approach is to control the particle size. Generally, the appropriate particle size can make lithium ion diffusion easy [9]. However, the carbon coating [10–12] and metal ion doping [13–15] were also used to enhance the properties

of  $\text{LiMnPO}_4$ . On the other hand, the electrochemical performance of  $\text{LiMnPO}_4$  can also be improved by the optimized synthesis route. Taking a example of sol–gel method [16], the precursor is dispersed into the molecular level in the solution and the gel can be obtained during stirring process. Meanwhile, chelating agent is adopted to form the gel in this system. Finally, the sintering temperature is lower compared with traditional solid state route, and the particle size is minimized.

In this work, olivine  $\text{LiMnPO}_4/\text{C}$  was synthesized via a sol–gel method based on the citric acid. The citric acid was used as chelating agent and carbon source in this route. As a chelating agent, the citric acid can help precursor to disperse into the molecular level in the solution. During the sintering process, the decomposition of citric acid could minimize the particle size of  $\text{LiMnPO}_4/\text{C}$ . The effects of sol–gel route on  $\text{LiMnPO}_4/\text{C}$  were measured by TG, XRD, SEM and electrochemical performance test. The optimal synthesis conditions of  $\text{LiMnPO}_4/\text{C}$  by sol–gel method could be defined from these results.

**Foundation item:** Project (0991025) supported by Natural Science Foundation of Guangxi, China; Project (51164007) supported by the National Natural Science Foundation of China; Project (201101ZD008) supported by Educational Commission of Guangxi, China

**Corresponding author:** LIU Jie-qun; Tel: +86-512-67164815; E-mail: [ljq@suda.edu.cn](mailto:ljq@suda.edu.cn)  
DOI: 10.1016/S1003-6326(11)61497-0

## 2 Experimental

The  $\text{LiMnPO}_4/\text{C}$  composite material was synthesized via a sol-gel method based on citric acid. The stoichiometric amounts of  $\text{Mn}(\text{CH}_3\text{COO})_2 \cdot 4\text{H}_2\text{O}$ ,  $\text{CH}_3\text{COOLi} \cdot 2\text{H}_2\text{O}$ ,  $\text{H}_3\text{PO}_4$  and citric acid were dissolved together in distilled water. The PEG400 was added into the aqueous solution. The pH of solution was controlled at 10 by  $\text{NH}_3 \cdot \text{H}_2\text{O}$ . With stirring at  $60^\circ\text{C}$ , the gel was obtained. After drying at  $60^\circ\text{C}$  for 48 h, the precursor powder was sintered at  $400\text{--}600^\circ\text{C}$  for 5–15 h under argon atmosphere.

Powder X-ray diffraction (XRD, X'Pert Pro) using  $\text{Cu K}\alpha$  radiation over the  $2\theta$  range of  $10^\circ\text{--}80^\circ$  with a step size of  $0.02^\circ$  was employed to identify the crystalline phase of the synthesized materials. The particle morphologies of the powders were observed using scanning electron microscope (SEM, JSM-6380LV). The electrochemical characterization was performed using CR2025 coin-type cell. For positive electrode fabrication, the prepared active material  $\text{LiMnPO}_4$  was mixed with 10% carbon black and 10% polyvinylidene fluoride in N-methyl pyrrolidinone until slurry was obtained. And then the blended slurry was pasted onto an aluminum current collector, and the electrode was dried at  $120^\circ\text{C}$  for 4 h in vacuum. The cathode were punched into circular discs with a diameter of 1.2 cm. The test cell consisted of the positive electrode and lithium foil negative electrode separated by a porous polypropylene film, and 1 mol/L  $\text{LiPF}_6$  in EC+EMC+DMC (1:1:1 in volume) as the electrolyte. The assembly of the cells was carried out in a dry Ar-filled glove box. The cells were charged and discharged over a voltage range of 2.75–4.50 V versus  $\text{Li}/\text{Li}^+$  electrode on a battery tester (BTS-5V3A) at 0.05C rate. The cyclic voltammogram (CV) was investigated by electro-chemical workstation (CHI660A). The CV was tested at a scanning rate of 0.1 mV/s in the voltage range of 2.5–4.5 V.

## 3 Results and discussion

### 3.1 TG-DTA curves of precursor

TG-DTA curves for the gel precursor operated at a temperature of  $25\text{--}1000^\circ\text{C}$  are shown in Fig. 1. As shown in DTA curve, an endothermic peak is observed at  $160^\circ\text{C}$ , due to the process about thermal decomposition of ammonium salt and organic matter. About 10% of mass loss is observed during the temperature sweep to  $160^\circ\text{C}$ . It can be seen that the mass loss is about 10% in the second mass loss temperature range of  $160\text{--}200^\circ\text{C}$ . In the temperature range, citric acid begins the decarboxylation reaction, which is an exothermic

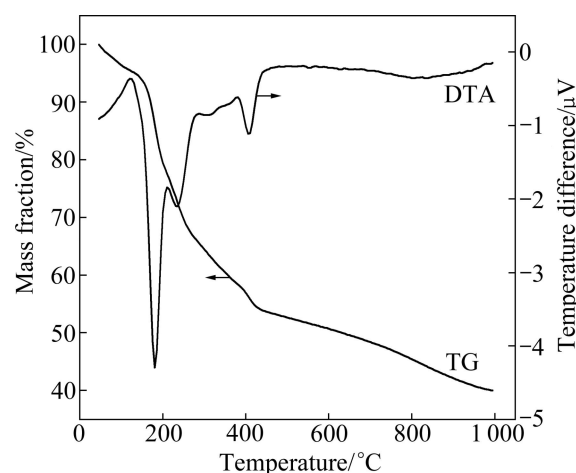


Fig. 1 TG-DTA curves of precursor

reaction. As temperature increases to  $300^\circ\text{C}$ , citric acid begins to burn and release heat. Therefore, a little exothermic peak can be observed at about  $300^\circ\text{C}$  in DTA curve. Meanwhile, about 20% of mass loss is yielded during this combustion process. When temperature increases to about  $400^\circ\text{C}$ ,  $\text{LiMnPO}_4/\text{C}$  is primarily formed and about 50% mass retains in the final product. So,  $\text{LiMnPO}_4/\text{C}$  begins to form at  $400^\circ\text{C}$ . It can be known that the synthesis temperature of  $\text{LiMnPO}_4/\text{C}$  is significantly reduced by sol-gel method.

### 3.2 XRD patterns of synthesized $\text{LiMnPO}_4/\text{C}$ samples

X-ray diffraction (XRD) was adopted to investigate the effects of different sintering temperatures and time on crystal structure of  $\text{LiMnPO}_4/\text{C}$ . Figure 2 shows the XRD patterns of  $\text{LiMnPO}_4/\text{C}$  samples calcined at different temperatures. The single olivine phase in  $\text{LiMnPO}_4$  can be observed in three XRD patterns, and no impurity peak

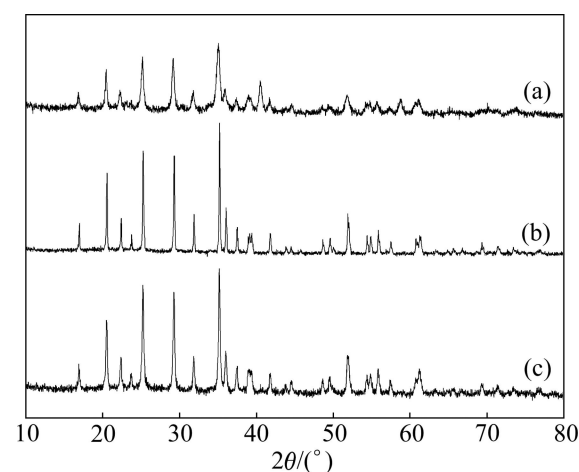
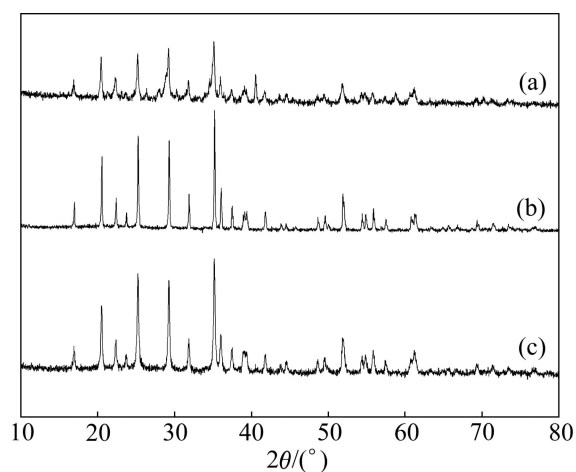


Fig. 2 XRD patterns of  $\text{LiMnPO}_4/\text{C}$  samples calcined at different temperatures for 10 h: (a)  $400^\circ\text{C}$ ; (b)  $500^\circ\text{C}$ ; (c)  $600^\circ\text{C}$

can be seen. Therefore, it is able to obtain the pure  $\text{LiMnPO}_4/\text{C}$  via a sol–gel route at three different temperatures. But, in Fig. 2(a), intensity of diffraction peaks is too low, resulting from the low temperature (e.g.  $400\text{ }^\circ\text{C}$ ) making a poor crystallinity of  $\text{LiMnPO}_4/\text{C}$ . The diffraction peaks of  $\text{LiMnPO}_4/\text{C}$  synthesized at  $500\text{ }^\circ\text{C}$  are sharper and narrower compared with others. Therefore, the well crystal structure of  $\text{LiMnPO}_4/\text{C}$  can be obtained at  $500\text{ }^\circ\text{C}$ . The precursor of  $\text{LiMnPO}_4$  is dispersed into the molecular level in sol–gel reaction. Then, in the sintering process, these uniform particles can be heated plenty and get a complete reaction.

Figure 3 illustrates that XRD patterns of  $\text{LiMnPO}_4/\text{C}$  samples calcined at  $500\text{ }^\circ\text{C}$  for different time. With increasing the calcination time, an apparent increase of intensity of diffraction peaks can be seen in Fig. 3. As shown in Fig. 1(a), intensity of diffraction peaks is low due to the fact that precursor powders cannot get enough time to form well crystal. Over calcination time of 10 h, the diffraction peaks of samples are sharp and narrow. Owing to the extension of sintering time,  $\text{LiMnPO}_4/\text{C}$  particles can crystallize perfectly.



**Fig. 3** XRD patterns of  $\text{LiMnPO}_4/\text{C}$  samples calcined at  $500\text{ }^\circ\text{C}$  for different time: (a) 5 h; (b) 10 h; (c) 15 h

### 3.3 SEM images of synthesized $\text{LiMnPO}_4/\text{C}$ samples

Figure 4 shows that SEM images of  $\text{LiMnPO}_4/\text{C}$  samples calcined at different temperatures for 10 h. In Fig. 4,  $\text{LiMnPO}_4/\text{C}$  particles gradually become larger when sintering temperature increases. This is attributed to that crystal particles grow so fast at high calcination temperature that large-sized particle can be obtained. As seen in Fig. 4(a),  $\text{LiMnPO}_4/\text{C}$  particles get incomplete growth at  $400\text{ }^\circ\text{C}$ . However, petal-like particles distribute evenly in Fig. 4(b). The decomposition of citric acid at  $500\text{ }^\circ\text{C}$  can improve the morphology of  $\text{LiMnPO}_4/\text{C}$ .  $\text{LiMnPO}_4/\text{C}$  particles obtained at  $600\text{ }^\circ\text{C}$  are

observed so much agglomeration that its conductivity will perform poor. The effects of calcination time on  $\text{LiMnPO}_4/\text{C}$  morphology are performed in Fig. 5. When calcination time is 5 h, particle sizes are large in Fig. 5(a). It is attributed to that the short calcination time is hard to form small and uniform particles, while long calcination time is not favor to the conformation of  $\text{LiMnPO}_4/\text{C}$  particles. The agglomeration can be observed in Fig. 5(c). However, optimal particles are distributed uniformly as Petal-shaped in Fig. 5(b). In summary, the  $\text{LiMnPO}_4/\text{C}$  sample synthesized at  $500\text{ }^\circ\text{C}$  for 10 h has the perfect crystal structure and morphology. The decomposition of citric acid can also control the particle size of  $\text{LiMnPO}_4/\text{C}$ . Lithium ion diffusion and conductivity of  $\text{LiMnPO}_4$  can be enhanced via the sol–gel route based on citric acid.

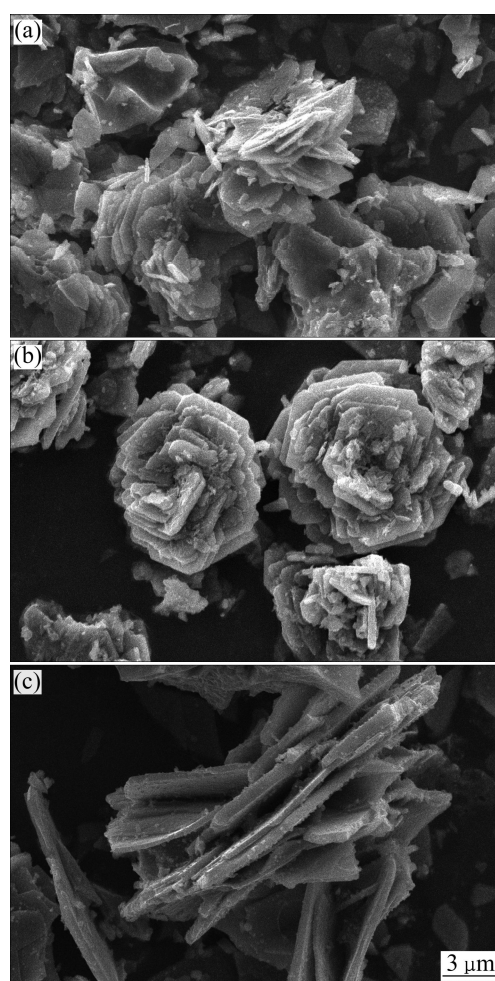


**Fig. 4** SEM images of  $\text{LiMnPO}_4/\text{C}$  samples calcined at different temperatures for 10 h: (a)  $400\text{ }^\circ\text{C}$ ; (b)  $500\text{ }^\circ\text{C}$ ; (c)  $600\text{ }^\circ\text{C}$

### 3.4 Electrochemical characteristics

The first charge–discharge curves of  $\text{LiMnPO}_4/\text{C}$  samples synthesized at different temperatures are

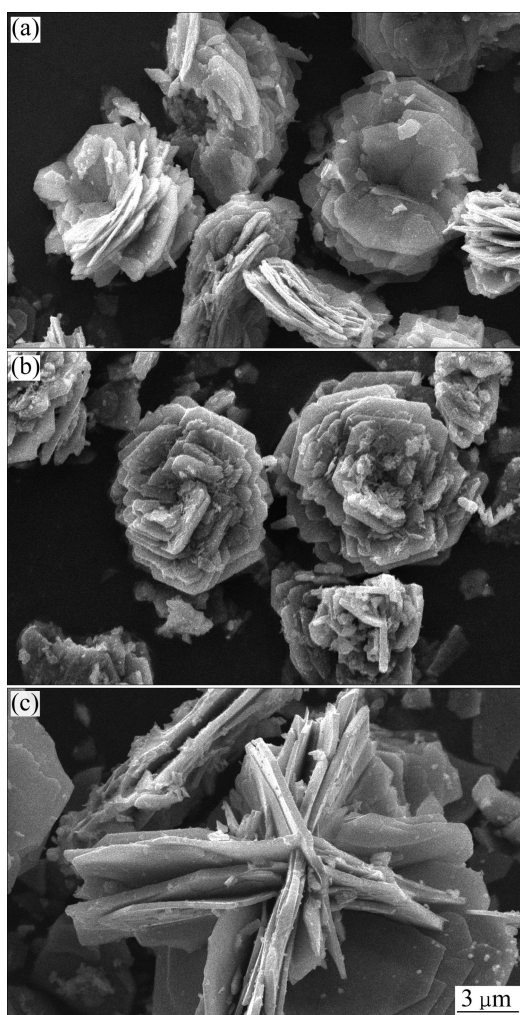


**Fig. 5** SEM images of  $\text{LiMnPO}_4/\text{C}$  samples calcined at  $500\text{ }^\circ\text{C}$  for different time: (a) 5 h; (b) 10 h; (c) 15 h

illustrated in Fig. 6. The  $\text{LiMnPO}_4/\text{C}$  samples demonstrate a reversible initial discharge capacity of  $110.8\text{ mA}\cdot\text{h/g}$  at  $400\text{ }^\circ\text{C}$ ,  $122.6\text{ mA}\cdot\text{h/g}$  at  $500\text{ }^\circ\text{C}$  and  $114.7\text{ mA}\cdot\text{h/g}$  at  $600\text{ }^\circ\text{C}$ . The cycling results of three samples are shown in Fig. 7. After 30 cycles, it retained  $112.4\text{ mA}\cdot\text{h/g}$  at  $500\text{ }^\circ\text{C}$ . The capacities of two other samples synthesized at  $400\text{ }^\circ\text{C}$  and  $600\text{ }^\circ\text{C}$  reduced so rapidly, and retained respectively  $100.3\text{ mA}\cdot\text{h/g}$  and  $104.3\text{ mA}\cdot\text{h/g}$  after 30 cycles.

The first charge–discharge curves of  $\text{LiMnPO}_4/\text{C}$  samples calcined at  $500\text{ }^\circ\text{C}$  with different calcination time are illustrated in Fig. 8. And the results of cycling performance are shown in Fig. 9. The curves present that the good charge–discharge performance is obtained for 10 h, such as the initial discharge capacity of  $122.6\text{ mA}\cdot\text{h/g}$  and residual capacity of  $112.4\text{ mA}\cdot\text{h/g}$  after 30 cycles. The  $\text{LiMnPO}_4/\text{C}$  sintered for 5 h has the initial discharge capacity of  $111.7\text{ mA}\cdot\text{h/g}$  and residual capacity of  $100.4\text{ mA}\cdot\text{h/g}$  after 30 cycles. However, the first

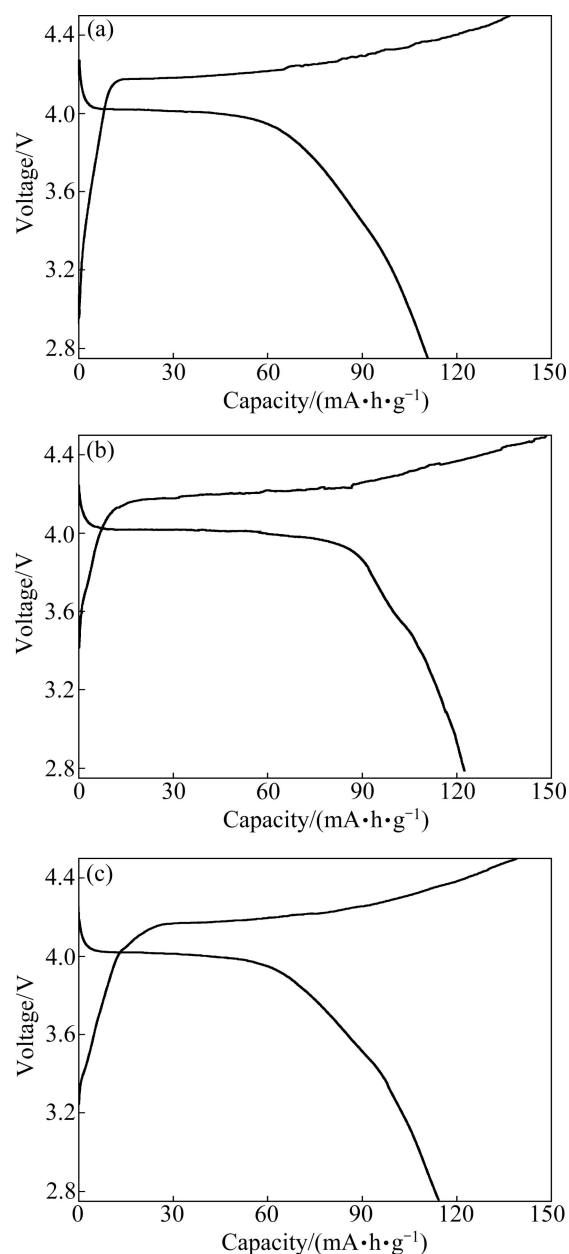


**Fig. 6** First charge–discharge curves of  $\text{LiMnPO}_4/\text{C}$  samples calcined for 10 h at different temperatures: (a)  $400\text{ }^\circ\text{C}$ ; (b)  $500\text{ }^\circ\text{C}$ ; (c)  $600\text{ }^\circ\text{C}$

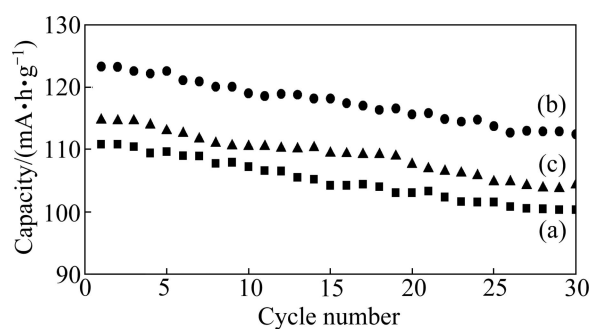


**Fig. 7** Electrochemical cycling performance of  $\text{LiMnPO}_4/\text{C}$  samples calcined for 10 h at different temperatures: (a)  $400\text{ }^\circ\text{C}$ ; (b)  $500\text{ }^\circ\text{C}$ ; (c)  $600\text{ }^\circ\text{C}$

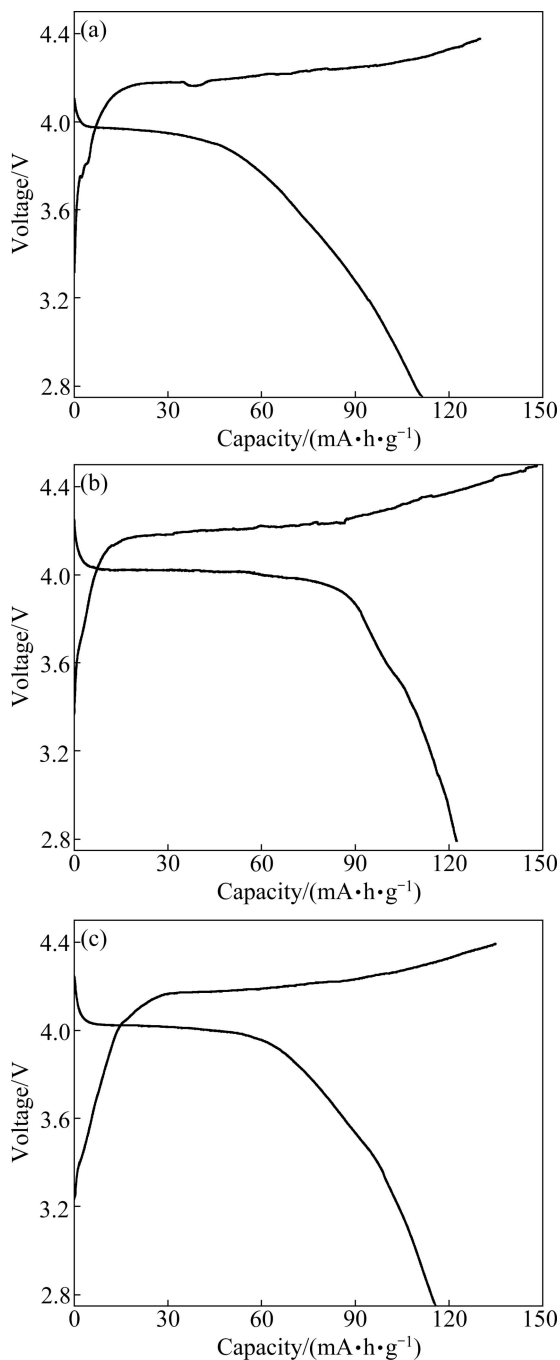


**Fig. 8** First charge–discharge curves of  $\text{LiMnPO}_4/\text{C}$  samples calcined at  $500\text{ }^\circ\text{C}$  for different time: (a) 5 h; (b) 10 h; (c) 15 h

discharge capacity of the sample calcined for 15 h is  $115.7\text{ mA}\cdot\text{h}/\text{g}$ , retains at  $104.5\text{ mA}\cdot\text{h}/\text{g}$  after 30 cycles.

The CV curves of  $\text{LiMnPO}_4/\text{C}$  are illustrated in Fig. 10. The reduction and oxidation peak positions of  $\text{LiMnPO}_4/\text{C}$  are located at  $3.957\text{ V}$  and  $4.362\text{ V}$ , and the difference between reduction and oxidation peak of  $\text{LiMnPO}_4/\text{C}$  is  $0.405\text{ V}$ . Carbon monoxide released by citric acid in sintering process can maintain the stability of  $\text{Mn}^{2+}$ . Hence, it reveals that  $\text{LiMnPO}_4/\text{C}$  prepared by sol–gel reaction has a good electrochemical reversibility.

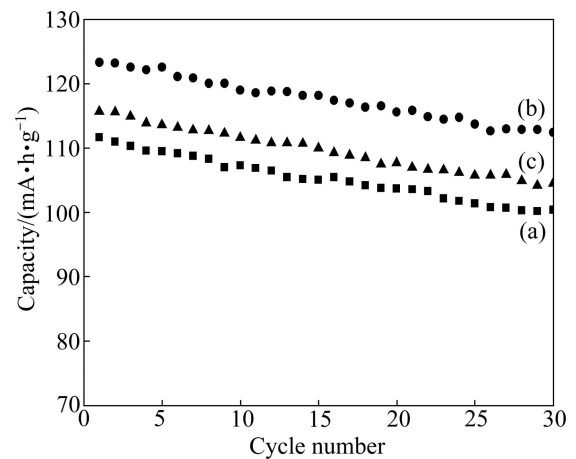


**Fig. 9** Electrochemical cycling performance of  $\text{LiMnPO}_4/\text{C}$  samples calcined at  $500\text{ }^\circ\text{C}$  for different time: (a) 5 h; (b) 10 h; (c) 15 h

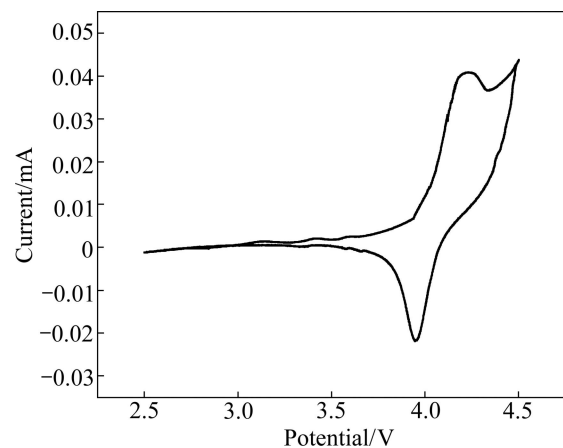


**Fig. 10** Cyclic voltammogram curve of  $\text{LiMnPO}_4/\text{C}$

## 4 Conclusions

1)  $\text{LiMnPO}_4/\text{C}$  cathode materials were synthesized via a sol–gel route based on citric acid.

2)  $\text{LiMnPO}_4/\text{C}$  synthesized at a low temperature of  $500\text{ }^\circ\text{C}$  for 10 h has an appropriate particle size, while the particle diameter is well-distributed. It performs the best discharge capacity of  $122.6\text{ mA}\cdot\text{h}/\text{g}$  at  $0.05\text{C}$  and the retaining capacity of  $112.4\text{ mA}\cdot\text{h}/\text{g}$  over 30 cycles. The CV shows a good electrochemical reversibility of  $\text{LiMnPO}_4/\text{C}$ .

3) The conductivity and reversibility of  $\text{LiMnPO}_4/\text{C}$  are commendably enhanced, by sol–gel route based on citric acid.

## References

- [1] PADHI A K, NANJUNDASWAMY K S, GOODENOUGH J B. Phospho-olivines as positive–Electrode materials for rechargeable lithium batteries [J]. *J Electrochem Soc*, 1997, 144(4): 1188–1194.
- [2] YIN Yan-hong, LI Shao-yu, YAN Lin-lin, ZHANG Hui-shuang,

- YANG Shu-ting. Modified carbothermal reduction method for synthesis of LiFePO<sub>4</sub>/C composite [J]. Transactions of Nonferrous Metals Society of China, 2012, 22(3): 621–626.
- [3] KANG B, CEDER G. Battery materials for ultrafast charging and discharging [J]. Nature, 2009, 458: 190–193.
- [4] GOODENOUGH J B, HONG H Y P, KAFALAS J A. Fast Na<sup>+</sup>-ion transport in skeleton structures [J]. Mater Res Bull, 1976, 11(2): 203–220.
- [5] BYKOV A B, CHIRKIN A P, DEMYANETS L N, DORONIN S N, GENKINA E A, IVANOV-SHITS A K., KONDRATYUK I P, MAKSIMOV B A, MELNIKOVA O K, MURADYAN L N, SIMONOV V I, TIMOFEEVA V A. Superionic conductors Li<sub>3</sub>M<sub>2</sub>(PO<sub>4</sub>)<sub>3</sub> (M=Fe, Sc, Cr): Synthesis, structure and electrophysical properties [J]. Solid State Ionics, 1990, 38(1–2): 31–52.
- [6] DOAN N L, TANIGUCHI I. Cathode performance of LiMnPO<sub>4</sub>/C nanocomposites prepared by a combination of spray pyrolysis and wet ball-milling followed by heat treatment [J]. J Power Sources, 2011, 196(3): 1399–1408.
- [7] DELACOURT C, LAFFONT L, BOUCHET R, WURM C, LERICHE J B, MORCRETTE M, TARASCON J M, MASQUELIER C. Toward understanding of electrical limitations (electronic, ionic) in LiMPO<sub>4</sub> (M=Fe, Mn) electrode materials [J]. J Electrochem Soc, 2005, 152(5): 913–921.
- [8] YONEMURA M, YAMADA A, TAKEI Y, SONOYAMA N, KANNO R. Comparative kinetic study of olivine LiMPO<sub>4</sub> (M= Fe, Mn) [J]. J Electrochem Soc, 2004, 151(9): 1352–1356.
- [9] WANG D Y, BUQA H, CROUZET M, DEGHENGI G, DREZEN T, EXNAR I, KWON N H, MINERS J H, POLETTO L, GRÄTZEL M. High-performance, nano-structured LiMnPO<sub>4</sub> synthesized via a polyol method [J]. J Power Sources, 2009, 189(1): 624–628.
- [10] SHIRATSUCHI T, OKADA S, DOI T, JAMAKI J. Cathodic performance of LiMn<sub>1-x</sub>M<sub>x</sub>PO<sub>4</sub> (M=Ti, Mg and Zr) annealed in an inert atmosphere [J]. Electrochim Acta, 2009, 54(11): 3145–3151.
- [11] DOMINKO R, BELE M, GABERSCEK M, REMSKAR M, HANZEL D, GOUPIL J M, PEJOVNIK S, JAMNIK J. Porous olivine composites synthesized by sol-gel technique [J]. J Power Sources, 2006, 153(2): 274–280.
- [12] CHEN G, WILCOX J D, RICHARDSON T J. Improving the performance of lithium manganese phosphate through divalent cation substitution [J]. Electrochem Solid-State Lett, 2008, 11(11): 190–194.
- [13] BRAMNIK N N, EHRENBERG H. Precursor-based synthesis and electrochemical performance of LiMnPO<sub>4</sub> [J]. J Alloys Compd, 2008, 464(1–2): 259–264.
- [14] LI G, AZUMA H, TOHDA M. LiMnPO<sub>4</sub> as the cathode for lithium batteries [J]. Electrochem Solid-State Lett, 2002, 5(6): 135–137.
- [15] MINAKSHI M, SINGH P, THURGATE S, PRINCE K. Electrochemical behavior of olivine-type LiMnPO<sub>4</sub> in aqueous solutions [J]. Electrochem Solid-State Lett, 2006, 9(10): 471–474.
- [16] PIANA M, CUSHING B L, GOODENOUGH J B, PENAZZI N. A new promising sol-gel synthesis of phospho-olivines as environmentally friendly cathode materials for Li-ion cells [J]. Solid State Ionics, 2004, 175(1–4): 233–237.

## 溶胶-凝胶法合成 LiMnPO<sub>4</sub>/C 锂离子电池复合材料

钟胜奎<sup>1,2,3</sup>, 王友<sup>2</sup>, 刘洁群<sup>1,2,3</sup>, 王健<sup>2</sup>

1. 桂林理工大学 广西建筑新能源与节能重点实验室, 桂林 541004;
2. 桂林理工大学 化学与生物工程学院, 桂林 541004;
3. 苏州大学 沙钢钢铁学院, 苏州 215021

**摘要:** 通过溶胶-凝胶法合成 LiMnPO<sub>4</sub>/C 锂离子电池复合材料, 采用 XRD、SEM 和电化学性能测试对 LiMnPO<sub>4</sub>/C 进行性能表征。XRD 研究表明, 在 500 °C 下能够合成得到纯的 LiMnPO<sub>4</sub>; SEM 研究表明, 柠檬酸作为螯合剂和碳源能有效地抑制 LiMnPO<sub>4</sub>/C 颗粒的长大。在 500 °C 下烧结 10 h 合成的 LiMnPO<sub>4</sub>/C 样品的电化学性能最好, 首次放电容量为 122.6 mA·h/g, 以 0.05C 倍率循环 30 次后其容量为 112.4 mA·h/g。

**关键词:** 锂离子电池; 正极材料; 溶胶-凝胶法; LiMnPO<sub>4</sub>/C; 电化学性能

(Edited by LI Xiang-qun)